Postwrinkling Behavior of a Conical Shell of Revolution Subjected to Bending Loads

G. A. GREENBAUM* AND D. C. CONROY†
TRW Systems Group, Redondo Beach, Calif.

An analysis and numerical method of solution are presented for determining the geometrically nonlinear behavior of a conical shell of revolution subjected to arbitrary loads. The analysis is based on Sanders' nonlinear shell theory. Expansion of all variables in a Fourier series in the circumferential coordinate reduces the governing nonlinear partial differential equations to a system of first-order ordinary differential equations. These equations are converted to a system of nonlinear algebraic equations by the use of the finite-difference method and are solved by a modified Newton iteration technique. Numerical results are presented for a postwrinkled pressurized cylindrical shell of revolution representing a typical tank section of the Atlas missile. The validity of this analysis is demonstrated by the very good correlation between the analytical and experimental results.

Nomenclature

$[A]$	=	matrix in Eq. (6)
$[A^*]$	=	matrix in Eq. (8)
D	=	extension stiffness
d	=	finite-difference interval size
E	=	Young's modulus
K	=	bending stiffness
L	=	defined in Eq. (4)
$[L]$	=	matrix defined by Eq. (12)
M	=	harmonic number
$M_\phi, M_\theta, M_{\phi\theta}$	=	bending and twisting moments
$N_\phi, N_\theta, N_{\phi\theta}$	=	inplane forces
$\bar{N}_{\phi\theta}$	=	boundary in-plane shear force
$\{P\}$	=	vector in Eq. (6)
$\{P^*\}$	=	vector in Eq. (8)
Q_ϕ, Q_θ	=	transverse forces
$\bar{Q}_\phi$	=	boundary transverse shear force
r	=	normal distance from the axis of revolution to a point on the shell
S	=	meridional coordinate
t	=	thickness
$[U]$	=	upper triangular matrix
u	=	circumferential displacement
v	=	meridional displacement
w	=	normal displacement
$\bar{X}, \bar{Y}, \bar{Z}$	=	surface loads, Fig. 1
$\{Y\}$	=	vector of the fundamental variables
$\{\Delta Y\}$	=	correction to the fundamental variables
μ	=	Poisson's ratio
$\omega, \omega_\phi, \omega_\theta$	=	surface rotations
ϕ	=	normal angle to the surface
θ	=	circumferential angle
θ_w	=	wrinkling angle

Subscripts

i	=	iteration number
M	=	harmonic index
n	=	pivotal point
q	=	segment number

Presented as Paper 69-90 at the AIAA 7th Aerospace Sciences Meeting, New York, January 20-22, 1969; submitted February 17, 1969; revision received September 22, 1969. The work reported in this paper was supported by NASA Langley Research Center under Contract NAS3-8704. The authors gratefully acknowledge the contributions made by A. Kaplan, D. A. Evensen, D. J. Peery, and R. Mancini.

* Section Head, Applied Mechanics. Member AIAA.
† Member of the Professional Staff.

I. Introduction

THIS paper presents an analysis and a numerical method for determining the elastic postwrinkling behavior of highly pressurized cylindrical and conical shells subject to axial compression and bending loads. It is well known that, for thin-walled pressurized cylinders subject to bending loads, the collapse load is considerably higher than the initial wrinkling load.[1,2] Weingarten et al.,[2] noted this result from their tests of mylar cylinders and cones; however, they pointed out that as the applied bending moment was increased, the depth of the wrinkles grew, and there was a possibility of fracturing the shell before the collapse load was attained. In practical pressure stabilized structures, such as the Atlas/Centaur vehicle, the presence of circumferential splice joints further increases the possibility of fracturing the cylinder. These joints form axisymmetric discontinuities and are the areas at which local wrinkling first occurs. Recent bending tests of the Atlas vehicle,[3] indicated that the Atlas could be loaded, without failure, well above the initial wrinkling load. These tests showed that as the bending moment was increased, deep wrinkles and large stresses developed around the circumferential splice joints. Therefore, before pressure-stabilized vehicles can be designed to achieve their full load-carrying capacity, a need existed to analytically determine their postwrinkling behavior. The primary objective of the present investigation is to provide the designer and stress analyst an analytical technique for determining the postwrinkling deformations, strains, and stresses of Atlas/Centaur type structures.

In order to achieve the stated objective, a numerical analysis and a computer program were developed to determine the nonlinear behavior of nonsymmetrically loaded shells of revolution. Numerous authors have formulated numerical techniques to obtain the linear behavior of nonsymmetrically loaded shells of revolution.[4-6] Some attention has been given to the nonlinear axisymmetrically loaded shell of revolution problem[7-9]; however, the nonlinear asymmetrically loaded shell of revolution has not received much attention. Famili and Archer[10] developed a numerical method for obtaining the finite asymmetric deformations of shallow spherical shells. Their technique consists of using a double finite-difference mesh, together with an iteration scheme, to determine the asymmetric postbuckling state for a spherical cap under uniform external pressure.

During the course of this investigation, the authors' attention was called to a recent report by Ball.[11] Ball uses a

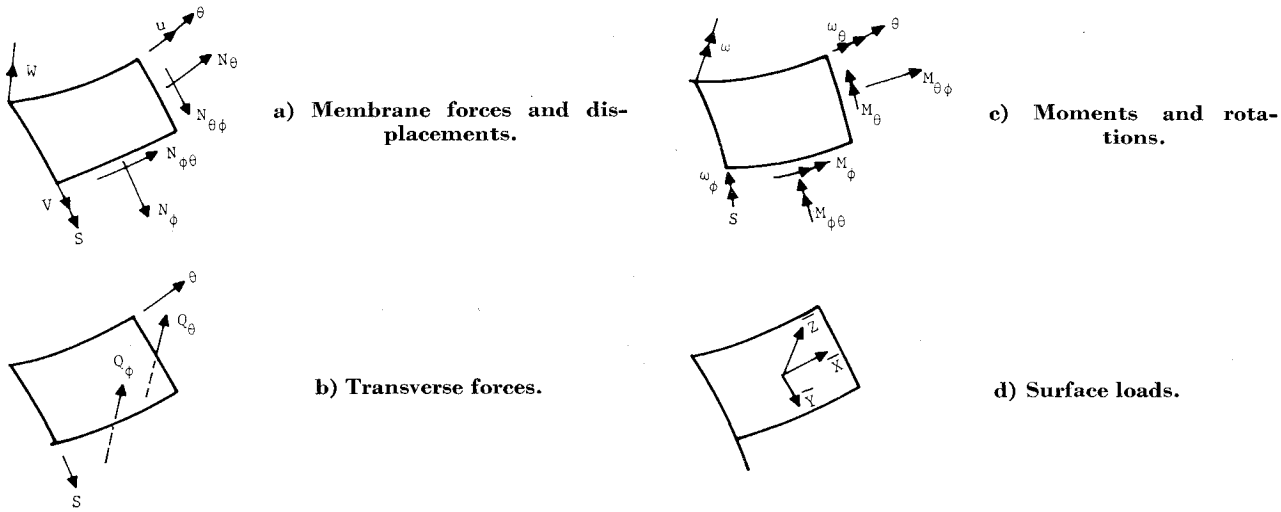

Fig. 1 Positive direction of the forces, moments, displacements, and loads acting on a shell element.

numerical technique similar to that presented here, but solves four second-order differential equations rather than the eight first-order equations as presented in this report. Ball also uses a different type of iteration technique than presented in this report. The authors found that Ball's technique did not converge for the postwrinkling problem.

The field equations used in this paper were derived by Sanders,[12] and are based on the assumptions of small strains and moderately small rotations. Following a method presented by Kalnins,[4] each of the variables is expanded in a Fourier series in the circumferential direction, and the field equations are reduced to eight nonlinear first-order differential equations. Unlike the linear theory, the equations for each harmonic do not uncouple when coefficients of like trigonometric arguments are collected together. The nonlinear terms involve products of series, hence the Fourier harmonics become coupled. The task of solving these equations in the coupled form would be an enormous undertaking because, for the solution of any practical problem, this would involve solving a very large-band matrix many times. For this reason, a numerical technique was developed whereby the harmonics are solved in an uncoupled form. Briefly, the solution technique consists of reducing the eight first-order differential equations to a system of nonlinear algebraic equations by the use of the finite-difference method. These equations are then solved by a modified Newton method. The modification of the Newton method consists of retaining only those nonlinear terms on the left side of the equations which do not couple harmonics; all other nonlinear terms are placed on the right side of the equations. An iteration method is then used on trial solution vectors until the solution converges. Experience in using this method has indicated that, at least for the class of problems considered here, the convergence properties are quite good.

To illustrate the application of the method developed in this report, and to verify the analytical method, the postwrinkling behavior of a portion of the Atlas vehicle was obtained. The analytical and experimental results are compared and found to be in close agreement.

II. Governing Shell Equations

Previous investigators,[6] and one of the present authors,[13] have solved the linear shell of revolution equations by reducing the field equations to four second-order differential equations in terms of u, v, w, and M_ϕ. In using this formulation, it was found that in certain classes of problems (specifically, problems involving large inextensional deformations), numerical inaccuracies occurred due to the subtraction of large numbers of nearly equal size. These inaccuracies occurred mostly in the calculation of forces and moments near discontinuities. In order to minimize these errors without having to resort to a computer program written entirely in double precision, the present formulation reduces the field equations to eight first-order equations in terms of the eight variables, u, v, w, ω_θ, $\bar{N}_{\phi\theta}$, N_ϕ, $\bar{Q}_\phi$, and M_ϕ. In this formulation, boundary conditions and discontinuity equations do not involve any derivatives. Experience with using the eight first-order equations indicates that the inaccuracies obtained with the four second-order equations were eliminated, and comparisons of results from the two formulations has shown that for the same number of pivotal points the eight first-order equations yield more accurate results.

The eight first-order equations have previously been used for solving linear shell problems.[4,5] These authors used a numerical integration technique to solve these equations. It was pointed out by Kalnins[4] that the numerical integration technique does have one serious liability; a loss of accuracy can result when the length of the shell increases. This inaccuracy results from the subtraction of almost equal numbers in the process of determining the boundary conditions; Kalnins showed that this inaccuracy could be minimized by segmenting the shell, and thereby, integrate only over short intervals. His method of solution consists of finding the influence coefficients for short intervals by numerical integration. After determining these quantities, continuity conditions on all variables at the ends of contiguous intervals are specified and constitute a set of simultaneous equations which are then solved. The finite-difference method does not have this type of inaccuracy problem, and for this reason was used in the present investigation.

The nonlinear shell of revolution field equations used in this paper were derived by Sanders,[12] and are valid for small stress and moderately small rotations. These equations are reduced to a system of eight first-order differential equations using a method similar to that given by Kalnins.[4] The complete derivations of the eight equations are given in Ref. 14, and hence will not be repeated here. The resulting equations are (see Fig. 1)

$$\bar{N}^{\cdot}{}_{\phi\theta} + 2\bar{N}_{\phi\theta}\cos\phi/r + N'_\theta/r + M'_\theta \sin\phi/r^2 - (\sin\phi/r)(N_{\phi\theta}\omega_\theta + N_\theta\omega_\phi) - [(N_\phi + N_\theta)\omega]\cos\phi/r + \bar{Z}\omega_\phi + \bar{X} = 0 \quad (1a)$$

$$N^{\cdot}{}_\phi + (N_\phi - N_\theta)\cos\phi/r + \bar{N}'_{\phi\theta}/r - 2M'_{\phi\theta}\sin\phi/r^2 + (1/r)[(N_\phi + N_\theta)\omega]' + \bar{Z}\omega_\theta + \bar{Y} = 0 \quad (1b)$$

$$\bar{Q}^{\cdot}{}_{\phi} + \bar{Q}_{\phi}\cos\phi/r - N_{\theta}\sin\phi/r + 2M'_{\phi\theta}\cos\phi/r^2 + M''_{\theta}/r^2 - (N_{\phi\theta}\omega_{\theta} + N_{\theta}\omega_{\phi})' + \bar{Z}(1 + \bar{\epsilon}_{\phi} + \bar{\epsilon}_{\theta}) = 0 \quad (1c)$$

$$M^{\cdot}{}_{\phi} + (M_{\phi} - M_{\theta})\cos\phi/r + 2M'_{\phi\theta}/r - \bar{Q}_{\phi} - (N_{\phi}\omega_{\theta} + N_{\phi\theta}\omega_{\phi}) = 0 \quad (1d)$$

$$u^{\cdot} + \frac{v'}{r} - \frac{u\cos\phi}{r} - \frac{2}{D(1-\mu)}\left[\bar{N}_{\phi\theta} - \frac{3}{2}M_{\phi\theta}\frac{\sin\phi}{r}\right] + \omega_{\phi}\omega_{\theta} + \frac{1}{D(1-\mu)}[(N_{\phi} + N_{\theta})\omega] = 0 \quad (1e)$$

$$v^{\cdot} - [1/D(1-\mu^2)](N_{\phi} - \mu N_{\theta}) + \tfrac{1}{2}(\omega_{\theta}^2 + \omega^2) = 0 \quad (1f)$$

$$W^{\cdot} + \omega_{\theta} = 0 \quad (1g)$$

$$\omega^{\cdot}{}_{\theta} - [1/K(1-\mu^2)](M_{\phi} - \mu M_{\theta}) = 0 \quad (1h)$$

where $(\ )^{\cdot} = \partial/\partial S$, $(\ )' = \partial/\partial\theta$ and the circumferential force N_{θ}, and moments M_{θ}, $M_{\phi\theta}$ are given by

$$N_{\theta} = \mu N_{\phi} + D(1-\mu^2)\times[(1/r)(v\cos\phi + u' + w\sin\phi) + \tfrac{1}{2}(\omega_{\phi}^2 + \omega^2)] \quad (2)$$

$$M_{\theta} = \mu M_{\phi} + \frac{K(1-\mu^2)}{r}\left[-\frac{w''}{r} + u'\frac{\sin\phi}{r} + \omega_{\theta}\cos\phi\right] \quad (3)$$

$$M_{\phi\theta} = \frac{K(1-\mu)}{2L}\left\{\frac{2\omega'_{\theta}}{r} + \frac{2w'\cos\phi}{r^2} - \frac{2v'\sin\phi}{r^2} - \frac{3}{2}\omega_{\phi}\omega_{\theta}\frac{\sin\phi}{r} + \frac{3\sin\phi}{D(1-\mu)r}\left[\bar{N}_{\phi\theta} - \frac{1}{2}(N_{\phi} + N_{\theta})\omega\right]\right\} \quad (4)$$

where $L = 1 + \frac{9}{4}(K/D)\sin^2\phi/r^2$.

Fourier Series Expansion

The derivatives of the variables with respect to the circumferential coordinate are eliminated by expanding the variables into Fourier series in the circumferential direction. In the present formulation, only symmetric loading about a meridional plane will be considered. For this case the variables have expansions of the form

$$\{\bar{X}, N_{\phi\theta}, \bar{N}_{\phi\theta}, Q_{\theta}, M_{\phi\theta}, u, \omega, \omega_{\phi}\} = \sum_{M=1}^{\infty}\{\bar{X}_M, N_{\phi\theta M}, \bar{N}_{\phi\theta M}, Q_{\theta M}, u_M, \omega_M, \omega_{\phi M}\}\{\sin M\theta\} \quad (5a)$$

$$\{\bar{Y}, \bar{Z}, N_{\phi}, N_{\theta}, Q_{\phi}, Q_{\phi}, M_{\phi}, M_{\theta}, v, w, \omega_{\theta}\} = \sum_{M=0}^{\infty}\{\bar{Y}_M, \bar{Z}_M, N_{\phi M}, N_{\theta M}, Q_{\phi M}, \bar{Q}_{\phi M}, M_{\phi M}, M_{\theta M} v_M, w_M, \omega_{\theta M}\}\times\{\cos M\theta\} \quad (5b)$$

If we substitute Eqs. (2–5) into Eqs. (1), and collect terms of like trigonometric arguments, the governing eight first-order differential equations for any harmonic M are obtained

$$\{Y\}^{\cdot}{}_M + [A]_M\{Y\}_M = \{P\}_M \quad (6)$$

where

$$\{Y\}_M{}^T = \{\bar{N}_{\phi\theta M}, N_{\phi M}, \bar{Q}_{\phi M}, M_{\phi M}, u_M, v_M, w_M, \omega_{\theta M}\}$$

and the coefficients of the matrix $[A]$ and right-hand vector $\{P\}$ are given in Ref. 14.

III. Solution Technique

Iterative Method

Equations (6) are a nonlinear set of first-order differential equations. Moreover, because of the nonlinear terms the equations for each Fourier index, M, are not uncoupled as is the case for the linear analyses. A number of iterative methods were investigated for solving these nonlinear equations. The simplest method, which was used by Ball,[11] considers the nonlinear terms as pseudo-loading terms. The solution for the nth + 1 iteration of the nonlinear equations is obtained by using the solution for the nth iteration to calculate the pseudo-load terms (i.e., the right-hand vector). In this technique, the equations for each Fourier index are uncoupled since the nonlinear terms are placed in the right-hand vector. Furthermore, this technique involves changing only the right-hand vector for each iteration and is therefore quite fast. The major disadvantage of this method is that it has extremely poor convergence properties and sometimes it will not converge at all. In fact, when this method was tried in the present investigation, it was found that the solution diverged.

Another iteration method for solving nonlinear equations is Newton's method.[15] In Newton's method, the solution of the equations is expressed as the sum of two parts. The first part is an assumed solution and the second part is a correction to the assumed solutions.

$$\{Y\} = \{Y\} + \{\Delta Y\} \quad (7)$$

Substituting $\{Y\}$ into the governing Eqs. (6), and neglecting terms which are nonlinear in ΔY yields a system of linear equations from which the corrections, ΔY, may be determined. This method usually has good convergence properties, but is quite time consuming since each iteration involves changing both the left and right sides of the governing equations. Furthermore, when this method is carried out, the left side of the equations involve coupled harmonic equations and therefore the complete set of equations must be solved simultaneously. The task of repeatedly solving these equations until the solution converges requires excessive computation time.

The method which was used in the present investigation is essentially a compromise between the two methods just given. In this method Eq. (7) is substituted into the governing equations (6); however, all terms which couple harmonics on the left side of the equations are omitted so that the equations remain uncoupled. Also, in the present method, although the right sides of the equations are recalculated after each iteration, the left sides of the equations are changed only after a specified number of iterations, i.e., when convergence of the solution becomes poor. This technique has been found to work quite well and exhibits good convergence properties. Brogan and Almroth[16] described a similar method at the same conference where the present paper was given.

Substituting Eq. (7) into Eqs. (6) and neglecting the nonlinear terms in Δu, Δv, etc., and all terms on the left side of the equations which couple Fourier harmonics, yields the following set of equations for any harmonic M:

$$\{\Delta Y^{\cdot}\}_M + [A^*]\{\Delta Y\}_M = \{P^*\}_M \quad (8)$$

where $\{\Delta Y\}_M$ is the vector of the corrections to the fundamental variables and $[A^*]$ is the matrix of coefficients whose terms are given in Appendix C of Ref. 14. The terms of the right-hand vector $\{P^*\}_M$ are the original governing differential equations.

Finite-Difference Representation

The governing first-order differential equations are now reduced to a system of algebraic equations by use of the finite-difference method. One method of solving simultaneous first-order differential equations is given by Fox.[17]

The first derivative of a variable at pivotal points, n and $n + 1$, may be expressed in terms of the variables at these

points by the following equation:

$$\tfrac{1}{2}(\Delta Y^{*}_{n+1} + \Delta Y^{*}_{n}) = (1/d)(\Delta Y_{n+1} - \Delta Y_n) + \epsilon \Delta Y_{n+1/2} \quad (9)$$

where $\epsilon = 0(d^2)$, and $d = S_{n+1} - S_n$. ϵ, the error term in Eq. (9) is of the order of magnitude of the spacing squared. By using Eq. (9) and neglecting ϵ, Eq. (8) may be replaced by the algebraic equations

$$\{\tfrac{1}{2}[A^*]_{n+1} + (1/d)[I]\}\{\Delta Y\}_{n+1} + \{\tfrac{1}{2}[A^*]_n - 1/d[I]\}\{\Delta Y\}_n = \tfrac{1}{2}\{P^*\}_n + \tfrac{1}{2}\{P^*\}_{n+1} \; (n = 1, 2, 3 \ldots n) \quad (10)$$

where for conciseness matrix notation has been used, and for convenience the subscript M, referring to the Fourier index, has been omitted. The subscripts n and $n + 1$ refer to the pivotal points, and specify the points at which $[A^*]$, $\{\Delta Y\}$, and $\{P^*\}$ are evaluated.

Equation (10) may be considered as the result of applying the differential equations at a point half-way between the pivotal points n and $n + 1$. If there are n pivotal points, there are $8n$ unknowns. The use of Eq. (10) at every internal half-way point gives $8(n - 1)$ equations; the remaining eight equations are obtained from the boundary conditions.

Solution of the Algebraic Equations

The manner by which the boundary conditions, discontinuity equations, and the eight equations at each interior point are cast into a complete set, and the method of solving these equations will now be discussed. In general, complicated shell problems possess discontinuities and therefore must be segmented as shown in Fig. 2a. The governing equations for each segment are obtained by subdividing the segment into small intervals as shown in Fig. 2b. Normally, smaller intervals are needed where rapid variations of the solution occur. Thus, in the computer program developed for this analysis, smaller intervals may be specified near discontinuity and boundary points.

The algebraic equations for any harmonic are placed in the form shown in Fig. 3. The first four equations correspond to boundary conditions for the first point of segment 1. The next $8(n - 1)$ equations (n = number of points in segment 1), are the interior point Eq. (10). Eight discontinuity equations are then used to connect segments 1 and 2, etc.

When the complete set of equations is written in matrix notation, it can be seen that all nonzero terms of the matrix cluster about the main diagonal. This type of matrix is called a band matrix, and may be rapidly solved by a computer. For the present formulation, each row of the matrix contains only 16 terms. Furthermore, there are a maximum of 11 nonzero terms to the left or right of the main diagonal.

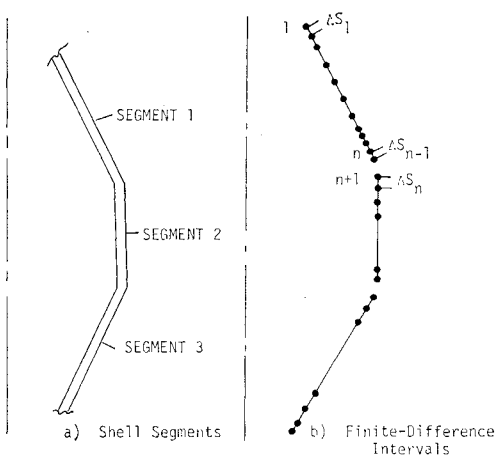

Fig. 2 Shell representation.

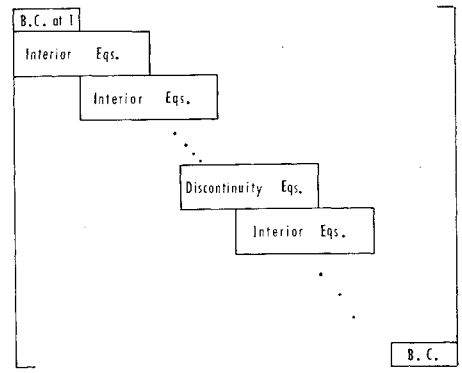

Fig. 3 Banded matrix of the governing equations.

Efficient computer storage may be obtained by storing the coefficients of this matrix in a rectangular array with the column of main diagonal terms placed in the middle of the array.

In the developed computer program, the gaussian elimination method[18] was used to solve the algebraic equations. This method will now be briefly described. Consider the system of simultaneous equations

$$[B]\{Y\} = \{F\} \quad (11)$$

where $[B]$ is a band matrix. The method of solving Eq. (11) for $\{Y\}$ is basically that of triangularizing $[B]$ by gaussian elimination. This is done by performing row operations on $[B]$ and $\{F\}$. Mathematically, this can be expressed by the multiplication of both sides of Eq. (11) by a matrix $[L]$ such that

$$[L][B] = [U] \quad (12)$$

where $[U]$ is an upper triangular matrix. Thus one obtains

$$[L][B]\{Y\} = [L]\{F\} \quad (13)$$

or

$$[U]\{Y\} = \{C\} \quad (14)$$

where

$$C = [L]\{F\} \quad (15)$$

Since $[U]$ is an upper triangular matrix, the solution of Eq. (14) is easily obtained by back substitution. By saving the upper triangular matrix $[U]$ and the matrix $[L]$, the solution for any new right-hand vector, $\{F\}$, may be rapidly determined.

In solving the nonlinear shell problem, the aforementioned method is used to obtain the corrections to the solution vector for each harmonic M. After a new solution for any harmonic has been obtained, it is used in the calculation of the new right-hand vectors for succeeding harmonics. This type of procedure is similar to a gauss-Seidel iteration method and was found to work quite well. A complete description of the iteration method will now be given.

Iteration Procedure

The technique for determining the nonlinear solution can best be described in a step-by-step manner. This will be done by outlining the technique used in the computer program developed for this investigation.

1) The first step toward obtaining the complete solution is to find the nonlinear solution due only to axisymmetric loading. The iterative method used for this case is essentially the Newton method. A linear solution to Eq. (10) is first obtained, for harmonic $M = 0$, by setting the prior solution equal to zero. This solution is then used to calculate the new right-hand vector and to rebuild the "A^*" coefficients.

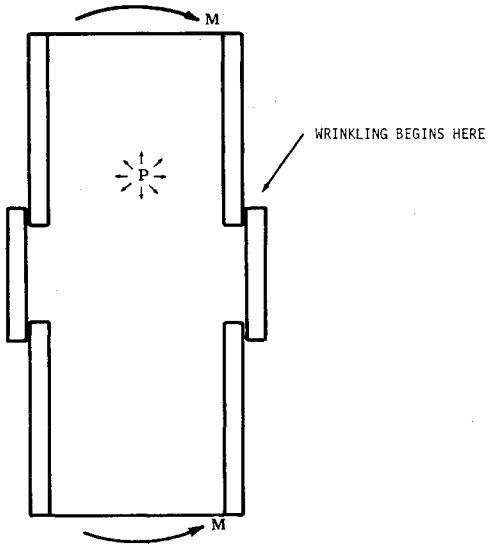

Fig. 4 Typical section of the Atlas missile.

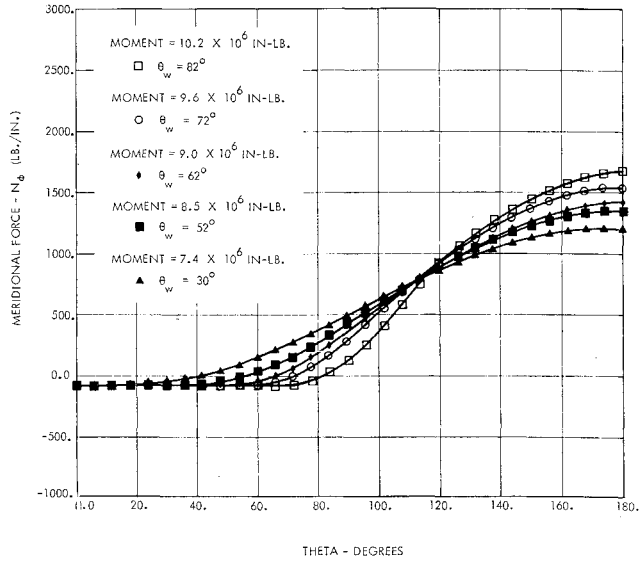

Fig. 6 Meridional forces vs circumferential coordinate.

The complete set of algebraic equations is then rebuilt and solved to obtain the corrections $\{\Delta Y\}$. This iterative technique (called a "special iteration") is repeated a specified number of times.

2) After the axisymmetric solution is obtained, it is used to calculate the A^* coefficients for all harmonics under consideration.

3) The governing equations for all harmonics are obtained and solved to determine the matrices $[U]$ and $[L]$. These matrices are retained so that the solution, due to any right-hand vector, may be easily obtained.

4) The next iterative step (called an "ordinary iteration") consists of determining the solution for each harmonic, starting with $M = 0$, for the first prescribed nonsymmetric load level. As the new solution for each harmonic is obtained, it is used to calculate the new right-hand vector for succeeding harmonics. When all harmonics have been processed, the corrections to the solutions for all harmonics are compared with the sum of the solutions of all harmonics. If the ratio is larger than a specified number, step 4 is repeated until either the solution satisfies the convergence criteria or a specified maximum number of iterations has been performed.

5) If the solution has not converged at this time, the program will print the results so far obtained and stop. Two choices are then available to the user. He may either reduce the load level and the magnitude of the loading increments and restart the program at step 4, or he may ask that the solution obtained at this time be used to rebuild the governing equations. If the latter case is used, the program may be restarted at step 2 (called an "update option"). Normally, the latter case is needed when large nonlinear deformations have occurred.

6) Finally, after the solutions have converged, the loading is increased and the procedure is repeated starting at step 4.

IV. Illustrative Problem

The present computer program (POWRS) was used to determine the postwrinkling behavior of a typical section (around Station 783.44), of the Atlas missile (Fig. 4). The cylindrical section is shown in Fig. 5a. The section consists of two cylinders joined together by an overlap splice joint. The model for this structure is shown in Fig. 5b. Basically, the model consists of three shell segments and two elastic rings joined to the cylinders at point c and d.

In determining the mathematical model for this structure, it was necessary to make a number of assumptions concerning

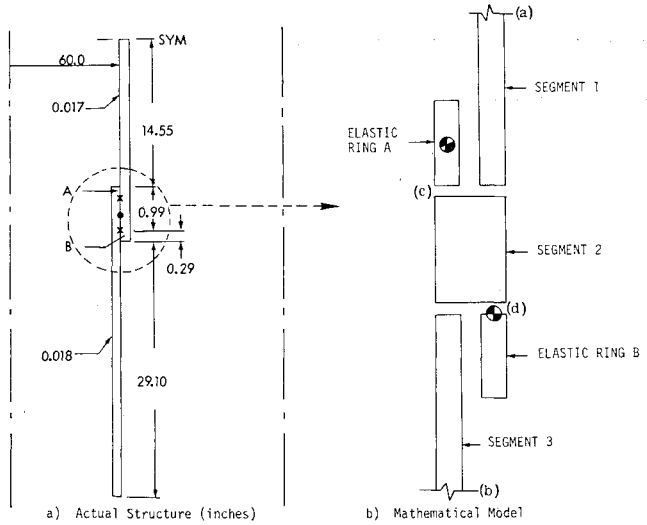

Fig. 5 Atlas section 738.44.

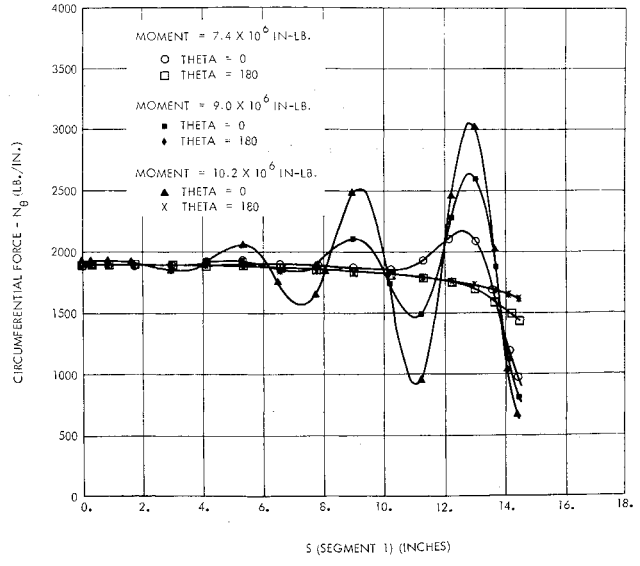

Fig. 7 Circumferential force vs meridional coordinate (segment 1).

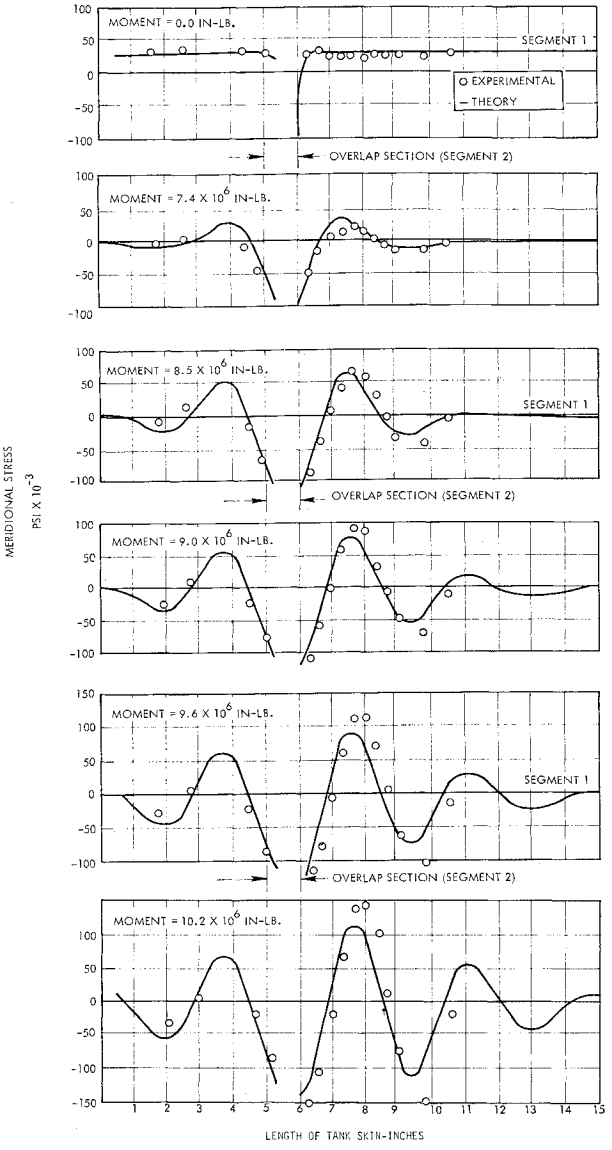

Fig. 8 Meridional stress vs S for $\theta = 0$.

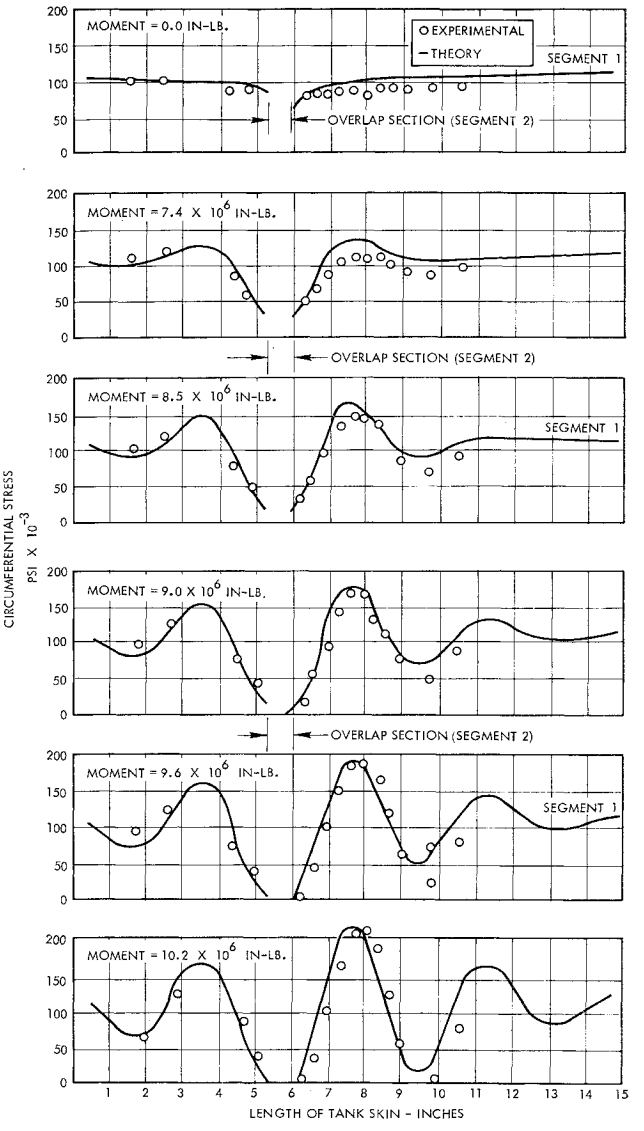

Fig. 9 Circumferential stress vs S for $\theta = 0$.

the short cylinders A and B (see Fig. 4a). Both cylinders were short enough so that they could be represented as elastic rings. Ring stiffness coefficients for these cylinders were obtained using the expressions given by Cohen.[19] However, when loaded, the two cylinders behave in different manners. Due to the external loads, cylinder A separates from the outside cylinder (segment 1), but cylinder B remains in contact with segment 3. The effect is that the forces acting on cylinder A are applied at discontinuity (c) which is offset from its c.g., but the resultant forces applied to cylinder B pass close to its c.g. To account for this difference, it was assumed that the c.g. of cylinder B was located at discontinuity (d), and the c.g. of cylinder A was taken as its geometric location. Although other mathematical models for this problem may be determined, it was felt that the present model would most closely represent the local behavior of this section.

A total of 137 pivotal points were used in the mathematical model of the structure. Segment 1 was divided into 50 intervals, segment 2 had 15 intervals, and segment 3 had 70 intervals. Small interval sizes were used near the discontinuity and boundary points because of the rapid variation of the solution in these areas.

The loading was identical to that of Ref. 3. The internal pressure at this section was 31.70 psi, the axisymmetric meridional load was 519 lb/in., and bending moments ranging from 0 to 10.2×10^6 in.-lb were applied to the section. The problem was solved in eight load steps starting at a moment of 7.4×10^6 in.-lb, and required 2.5 hr if IBM 7094 Mod II machine time to obtain the complete solution history. The time to obtain a solution for each load step varied from 10 min for a moment of 7.4×10^6 in.-lb to 20 min for a moment of 10.2×10^6 in.-lb.

The boundary conditions at point "a" corresponded to symmetry conditions. Boundary conditions at point b corresponded to a rigid ring which, prior to being loaded by a bending moment, was allowed to deform radially due to the pressure loading. The bending moment and axial load were applied to the rigid ring at point b. A total of seven Fourier harmonics were used in this analysis (i.e., $M = 0$ through $M = 6$).

An approximate analysis for predicting the over-all behavior of the postwrinkled Atlas missile was given by Peery.[20] This analysis assumes that the external moment is resisted by a meridional force which has a "$\cos\theta$" variation

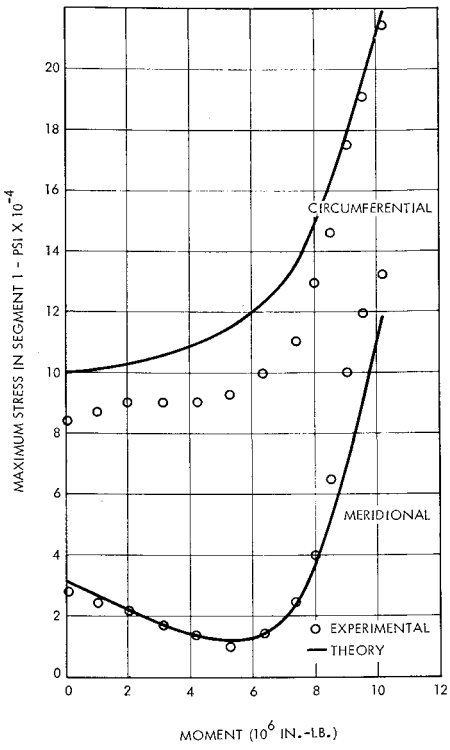

Fig. 10 Maximum stress in segment 1 vs applied moment.

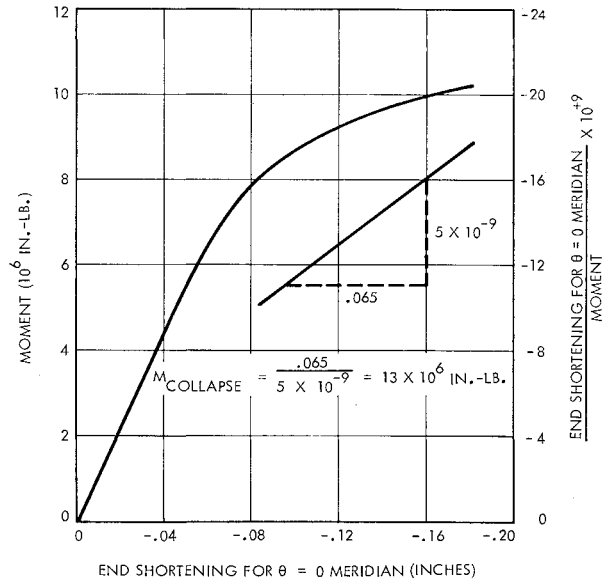

Fig. 11 Moment vs end shortening.

in the unwrinkled part of the cross section of the cylinder, and a constant meridional force equal to the critical compressive force

$$N_C = \{1/[3(1 - \varphi^2)]^{1/2}\}Et^2/r \qquad (16)$$

in the wrinkled area. Wrinkling of the cylindrical section is assumed to occur when the compressive meridional force equals N_C. For the present problem, this would occur at a bending moment of 6.75×10^6 in.-lb. It was found from the tests of Ref. 3, and the analysis given here, that this was a good representation of the way the cylinder behaved.

Figure 6 shows the circumferential variation of the meridional force in segment 1 for increasing values of the bending moment. These curves show the circumferential growth of the wrinkling angle, θ_w, as the load increases. Values of the wrinkling angle determined by Peery[20] are also shown. This angle is determined from the equation

$$\frac{M_B}{P_1 r} = \frac{(\pi - \theta_w) + \sin\theta_w \cos\theta_w}{2[\sin\theta_w + (\pi - \theta_w)\cos\theta_w]} \qquad (17)$$

where M_B = bending moment, $P_1 = 2\pi r(N_\phi + N_C)$, N_ϕ = axisymmetric meridional force.

Figure 7 gives the meridional variation of the circumferential force N_θ, in segment 1, for two circumferential angles. Since the circumferential force behaves similarly to the radial deformation, these curves reflect the growth of the deep wrinkles along the meridian and around the circumference of the shell. Theta equal to 0 corresponds to the maximum compressive force meridian.

Meridional and circumferential stresses obtained from the present analysis and the test of Ref. 3 (see Ref. 21) are shown in Figs. 8 and 9. The comparisons at intermediate values of the bending moment are quite good considering that at bending moments greater than 7.4×10^6 in.-lb, a 5% error in the applied moment causes a 20% error in stresses. The discrepancy in the circumferential stress away from the joint at zero moment could not be explained. Theoretically, the stress should have been a pure membrane stress of 112,000 psi and the low value given by the test must be attributed to experimental errors. The difference in results at high values of the bending moment were probably due to the nonlinearity of the material properties. The cylinders were made of 301 EH stainless steel which exhibits a large nonlinear stress-strain relationship above 160,000 psi. One can therefore expect that at bending moments greater than 8.5×10^6 in.-lb, the experimental results should give higher strains, and therefore higher stresses, when the data is reduced using a linear stress-strain law. Another possible reason for some difference in analytical and experimental results is that 301 EH stainless steel has a different modulus of elasticity in the meridional and circumferential direction while the present analysis assumes an isotropic homogeneous material.

The analysis showed that the maximum stress occurred on the outside surface of segment 1 at a distance of 1.7 in. from the discontinuity point c. Figure 10 shows the analytical and experimental stresses at this point. The stresses at this point do become quite high, and thus the cylinder may indeed rupture before the collapse load is attained.

Finally, Fig. 11 gives the end shortening of the $\theta = 0$ meridian as a function of the applied bending moment. An estimate of the collapse load of the cylinder may be obtained from this curve by using the Southwell method. Plotting δ/M vs δ as shown in Fig. 11 and taking the inverse of the slope of the resulting curve gives a collapse load of 13.0×10^6 in./lb. This value is only slightly below Peery's results which predicts that collapse occurs when the complete cylindrical cross section is wrinkled (i.e., $\theta_w = \pi$), and yields a collapse moment of 13.5×10^6 in./lb.

References

[1] Stein, M. and Hedgepath, J. M., "Analysis of Partly Wrinkled Membranes," TN D-813, July 1961, NASA.

[2] Weingarten, V. I., Morgan, E. J., and Seide, P., "Final Report on Development of Design Criteria in Elastic Stability of Thin Shell Structures," TR-60-000-9425, Dec. 1960, TRW Systems, Redondo Beach, Calif.

[3] Miller, R. P. and Gerus, T., "Bending Strength of a Large Thin-Walled Pressure-Stabilized Cylinder Beyond Onset of Compressive Skin Wrinkling," TM X-1311, Nov. 1966, NASA.

[4] Kalnins, A., "Analysis of Shells of Revolution Subjected to Symmetrical and Nonsymmetrical Loads," *Journal of Applied Mechanics*, Vol. 33, 1964, pp. 467–476.

[5] Cohen, G. A., "Computer Analysis of Asymmetrical Deformation of Orthotropic Shells of Revolution," *AIAA Journal*, Vol. 2, No. 5, May 1964, pp. 932–934.

[6] Budiansky, B. and Radkowski, P. P., "Numerical Analysis of Unsymmetrical Bending of Shells of Revolution," *AIAA Journal*, Vol. 1, No. 8, Aug. 1963, pp. 1833–1842.

[7] Bushnell, D., "Nonlinear Axisymmetric Behavior of Shells of Revolution," *AIAA Journal*, Vol. 5, No. 3, March 1967, pp. 432–439.

[8] Archer, R. R., "On the Numerical Solution of the Nonlinear Equations for Shells of Revolution," *Journal of Mathematics and Physics*, Vol. 41, 1962, pp. 165–178.

[9] Thurston, G. A., "A Numerical Solution of the Nonlinear Equations for Axisymmetric Bending of Shallow Spherical Shells," *Journal of Applied Mechanics*, Vol. 28, 1961, pp. 557–562.

[10] Famili, J. and Archer, R., "Finite Asymmetric Deformations of Shallow Spherical Shells," *AIAA Journal*, Vol. 3, No. 3, March 1965, pp. 506–510.

[11] Ball, R. E., "A Geometrically Nonlinear Analysis of Arbitrarily Loaded Shells of Revolution," NASA Contract NAS 1-5804, July 1967, Dynamic Science Corp.

[12] Sanders, J. L., "Nonlinear Theories for Thin Shells," *Quarterly of Applied Mathematics*, Vol. 21, 1963, pp. 21–36.

[13] Greenbaum, G. A. and Hubka, R. E., "Elastic Stress States and Natural Frequencies of Shells of Revolution Subjected to Unsymmetrical Loading," TRW Systems, Redondo Beach, Calif.

[14] Greenbaum, G. A. and Conroy, D. C., "Post-Wrinkling Analysis of Highly Pressurized Cylindrical and Conical Shells of Revolution Subjected to Bending Loads," Rept. 07823-6011-R000, Oct. 1967, TRW Systems, Redondo Beach, Calif.

[15] Thurston, G. A., "Newton's Method Applied to Problems in Nonlinear Mechanics," *Journal of Applied Mechanics*, Vol. 32, 1965, pp. 383–388.

[16] Brogan, F. A. and Almroth, B. O., "Buckling of Cylinders with Cutouts," AIAA Paper 69-92, New York, 1969.

[17] Fox, L., *The Numerical Solution of Two-Point Boundary Problems in Ordinary Differential Equations*, Oxford University Press, London, 1967.

[18] Osborne, E. E., "Direct Solution of Linear Algebraic Equations Involving an Almost Band Matrix of Large Order," Rept. NN158, 1961, TRW Systems, Redondo Beach, Calif.

[19] Cohen, G. A., "Computer Analysis of Asymmetric Free Vibrations of Ring-Stiffened Orthotropic Shells of Revolution," *AIAA Journal*, Vol. 3, No. 12, Dec. 1965, pp. 2305–2312.

[20] Peery, D. J., "Post-Buckling Strength of a Pressurized Cylinder," Convair, Rept. GD/A 63-0767, Nov. 1963, General Dynamics, San Diego, Calif.

[21] Miller, R. P., private communication.

APRIL 1970 AIAA JOURNAL VOL. 8, NO. 4

Bifurcation Type Buckling of Generally Orthotropic Clamped Plates

HARVEY R. FRASER JR.*
IBM, Hopewell Junction, N. Y.

AND

ROBERT E. MILLER†
University of Illinois, Urbana, Ill.

The objective of this investigation was to determine analytically the buckling loads for generally orthotropic, rectangular, flat, thin plates. The generalized Ritz method using a complete Fourier series with the Lagrange multiplier technique of minimization is used to compute upper and lower bounds of the bifurcation type buckling load. It is demonstrated that the generalized Ritz method is limited in a direct approach to clamped generally orthotropic plates. However, by utilizing an extended plate technique this method can be used to obtain solutions for generally orthotropic plates with three clamped edges. Several curves are generated that demonstrate the importance of the mechanical properties on uniaxial compression and shear buckling of clamped generally orthotropic plates.

Nomenclature

U = strain energy of plate
Ω = potential energy of applied loads
V = total potential energy
G = augmented total potential energy
θ = angle of inclination of plane of material symmetry
N = buckling parameter described in Fig. 1
N_x, N_y, N_{xy} = applied edge loads
a = length of plate
b = width of plate
$D_{11}, D_{22}, D_{12}, D_{66}, D_{16}, D_{26}$ = flexural rigidities
w = normal displacement
$a_{mn}, b_{mn}, c_{mn}, d_{mn}$ = generalized coordinates—coefficients of Fourier series, defined by Eq. (4)
δ_{on} = Kronecker delta
A_{mn}, B_{mn} = collection of terms in potential energy
D = $4A^2_{mn} - B^2_{mn}$
$\beta_n, \alpha_n, \eta_n, \gamma_n, \theta_n, \lambda_n, \mu_n, \phi_n$ = Lagrange multipliers

Received February 6, 1969; revision received August 5, 1969. This paper is based on a thesis submitted in partial fulfillment for the requirements of the Ph.D. degree in Theoretical and Applied Mechanics at the University of Illinois, Urbana, Ill.

* Staff Engineer, Components Division, East Fishkill Facility.
† Professor, Theoretical and Applied Mechanics Department. Member AIAA.

Introduction

THE increased interest in fiber reinforced plastics by the aerospace and electrical industries demands a better understanding of the strengths and weaknesses of this composite material. This paper focuses on the analysis of the bi-